SOURCE: CMOTT-91-06

On the Basic Equations for the Second-order Modeling of Compressible Turbulence

W. W. Liou and T.-H. Shih
Center for Modeling of Turbulence and Transition
ICOMP/NASA Lewis Research Center
Cleveland, OH 44135

Abstract

Equations for the mean and the turbulence quantities of compressible turbulent flows are derived in this report. Both the conventional Reynolds average and the mass-weighted Favre average were employed to decompose the flow variable into a mean and a turbulent quantities. These equations are to be used later in developing second-order Reynolds stress models for high-speed compressible flows. A few recent advances in modeling some of the terms in the equation due to compressibility effects are also summarized.

AIAA-91-1801-CP

UNSTABLE VISCOUS WALL MODES IN ROTATING PIPE FLOW

Z. Yang*
Center for Modeling of Turbulence and Transition
ICOMP, NASA Lewis Research Center
Cleveland, OH 44135

S. Leibovich†
Sibley School of Mechanical and Aerospace Engineering
Cornell University
Ithaca, NY 14853

Abstract

Linear stability of flow in rotating pipe is studied. These flows depend on two parameters, which can be taken as the axial Reynolds number Re and the rotating rate, q. In the region of $Re \gg 1$ and $q = O(1)$, the most unstable modes are concentrated near the pipe wall, the so-called "wall" modes. These wall modes are found to satisfy a simpler set of equations containing two parameters rather than four parameters as in the full linear stability problem. The set of equations is solved numerically and asymptotically over a wide range of the parameters. In the limit of $Re \to \infty$, the eigenvalue goes to the inviscid limit. The eigenfunction shows a two layer structure. It reaches the inviscid limit over the main part of the domain, while near the wall of the pipe, the eigenfunction is represented by a viscous solution of boundary layer type.

1. Introduction

Swirling flow is common in nature and technology. Fully-developed flow in a rotating pipe is an exact solution of the Navier-Stokes equations, and is the simplest available model of swirling flows. Swirling flows are known to be subject to instability, and the question of stability of flow in rotating pipe has consequently attracted a reasonable amount of attention. Pedley[1] showed that these flows are unstable to inviscid non-axisymmetric perturbations when the rotation is fast (in a sense which will made definite). Stability to inviscid perturbations in the finite rotation rate region was studied numerically by Maslowe[2]. Later, Maslowe and Stewartson[3] extended this work in a significant way and established by asymptotic methods that the dominant unstable modes are wall modes (that is, modes of motion concentrated asymptotically close to the wall) in the limit of large azimuthal wave number.

For viscous perturbations, Pedley[4], and simultaneously Jesoph and Carmi[5] found that the critical Reynolds number at which the perturbation is neutral in the limit of fast rotation. Cotton and Salwen[6] carried out comprehensive computations in search of neutral stability curves and they discovered that the neutral modes are center modes when Reynolds number is large. Center modes in rotating pipe flow were later analyzed asymptotically by Stewartson, Ng and Brown[7], and these authors speculated that center modes dominate for large Reynolds number.

In this study, we investigate the effect of viscosity on the inviscid wall modes found by Maslowe and Stewartson[3] when the Reynolds number is large but finite. We find the proper scaling for Reynolds number in order for viscous wall mode to exist and derive simplified governing equations for them. These equations contain only two parameters instead of four parameters in the full linear stability problem. The wall mode equations are then solved both numerically and asymptotically.

The plan of this study is as follow: Linear stability analysis is formulated in section 2, where it is shown numerically that the most unstable modes are wall modes. The governing equations for viscous wall modes are derived in section 3. Numerical solutions of the viscous wall mode equations are presented in section 4. An asymptotic analysis for the viscous wall modes equations is carried out in section 5, and section 6 concludes the paper.

2. Linear Stability Formulation

If length is nondimensionalized by the radius of the pipe L and velocity by the the axial velocity at the axis U, the laminar base flow in a pipe rotating with

*Research Associate
†Professor

angular velocity Ω is then described in a cylindrical (x, θ, r) coordinate system by,

$$\mathbf{U} = (1 - r^2, q\,r, 0) \tag{1}$$

where the inverse Rossby number

$$q = \frac{\Omega L}{U} \tag{2}$$

measures the relative strength of rotation. This nondimensionalization also defines a Reynolds number

$$Re = \frac{U L}{\nu} \tag{3}$$

where ν is the kinematic viscosity of the fluid.

Linear stability analysis concerns the stability of the motion subject to infinitesimal perturbations. Since the linear stability problem with base flow given by (1) is then separable in the x and θ directions, the perturbation field may be written in the normal mode form. i.e.

$$A\,[u(r), v(r), w(r), p(r)]exp\,[i(kx + m\theta - \omega t)]$$

where A is an arbitrary constant, k is the axial wave number of the perturbation and m is the azimuthal wave number of the perturbation. ω is the complex frequency, with its real part being the frequency and the imaginary part being the growth rate. Without loss of generality, m is taken as positive, k is any real number, and ω is to be found. If $\mathrm{Im}(\omega)$ is positive, the flow is linearly unstable.

The Navier-Stokes equations linearized about the base flow, and the equation of continuity are of the following form in the cylindrical coordinate system used,

$$i\gamma u - 2rw + ikp = \frac{1}{Re}\left(\frac{\partial^2 u}{\partial r^2} + \frac{1}{r}\frac{\partial u}{\partial r} - \frac{m^2}{r^2}u - k^2 u\right)$$

$$i\gamma v + 2qw + \frac{imp}{r} = \frac{1}{Re}\left(\frac{\partial^2 v}{\partial r^2} + \frac{1}{r}\frac{\partial v}{\partial r} - \frac{m^2+1}{r^2}v + \frac{2imw}{r^2} - k^2 v\right)$$

$$i\gamma w - 2qv + \frac{\partial p}{\partial r} = \frac{1}{Re}\left(\frac{\partial^2 w}{\partial r^2} + \frac{1}{r}\frac{\partial w}{\partial r} - \frac{m^2+1}{r^2}w - \frac{2imv}{r^2} - k^2 w\right)$$

$$iku + \frac{im}{r}v + \frac{\partial w}{\partial r} + \frac{w}{r} = 0 \tag{4}$$

where

$$\gamma = k(1 - r^2) + m\,q - \omega$$

The above equations for the perturbations are supplemented by the following boundary conditions. On the wall of the pipe, the no slip boundary conditions require

$$u(1) = v(1) = w(1) = 0 \tag{5}$$

At the center of the pipe, the perturbation must satisfy the following conditions to ensure that to be single-valued[8]

for $m = 0$

$$u'(0) = v(0) = w(0) = p'(0) = 0,$$

for $|m| = 1$

$$u(0) = v(0) + im\,w(0) = p(0) = 0,$$

for m otherwise

$$u(0) = v(0) = w(0) = p(0) = 0. \tag{6}$$

The above ordinary differential equations (4) and the boundary conditions (5) and (6) form an eigenvalue problem with ω as the eigenvalue. Nontrivial solution exists only when ω takes some specific values given by

$$\omega = \omega(Re, q; m, k)$$

If $\mathrm{Im}(\omega)$ is less than zero, the flow is stable; if $\mathrm{Im}(\omega)$ is positive, the flow is said to be linearly unstable. We are interested in the regions where the instability occurs. Earlier studies show, and our results confirm, that instability occurs only for $mk < 0$. In the following, we will take m positive, and k negative.

The linear stability problem was studied extensively by numerical means by Cotton and Salwen[6] and by Yang[9]. Cotton and Salwen searched in the parameter space $(Re, q; m, k)$ for the neutral modes (modes with zero ω_i), and found that the neutral modes are center modes, with most of the nontrivial activities confined near the center of the pipe. Yang's study concentrated on the most unstable modes, and we shall briefly describe the most unstable modes that he found in the region $Re \gg 1$ and $q = O(1)$.

Table 1 gives the information for the most unstable modes at $Re = 10000$ and some different values of q's. As q is increased, the the most unstable mode has larger values of both the azimuthal and axial wave numbers. In addition, we find for $q = O(1)$, although the real part and the imaginary part of the eigenvalue have quite different size, the difference of the real part of the eigenvalue from mq is of the same order as that of the imaginary part. These findings

Table 1: The most unstable modes for different q's with $Re = 10000$.

m: the azimuthal wave number,

k: the axial wave number,

ω: the eigenvalue of the most unstable mode.

q	m	k	ω
0.5	3	-0.50	(1.25, 0.177)
1.0	5	-0.81	(4.67, 0.296)
1.5	7	-1.04	(10.13, 0.379)
2.0	9	-1.20	(17.61, 0.439)
3.0	11	-1.22	(32.63, 0.518)

suggest the viscous wall mode scalings studied in the next section. For $q = 3$, the most unstable mode has the wave numbers $m = 11, k = -1.22$. The eigenfunction corresponding to this most unstable mode is shown in Fig 1. The eigenfunction is normalized such that the maximum axial velocity is 1. The real part of the eigenfunction is drawn in solid lines, and the imaginary part is drawn in dotted lines. The nontrivial behavior of this eigenfunction takes place in a thin region near the wall of the pipe. This behavior justifies the "wall mode" terminology used, and will be the subject of further study in next section.

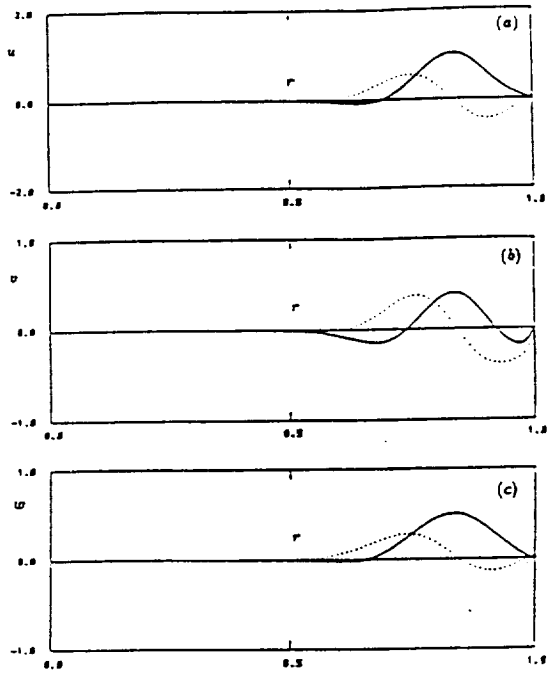

Figure 1: Eigenfunction for $Re = 10000, q = 3, m = 11, k = -1.22$. (a) axial velocity, (b) azimuthal velocity, (c) radial velocity.

3. The viscous wall mode equation

From the numerical computations in the last section, it is clear that in the region of $Re \gg 1$ and $q = O(1)$, the dominant modes are given by the asymptotic wall modes, a type of modes with large azimuthal wave number and with nontrivial behavior concentrated near the wall.

When azimuthal wave number m is large, there could be another type of mode for general swirling flows, the ring mode, as demonstrated by Leibovich and Stewartson[10]. In the case of rotating pipe flow, ring modes do not exist. Because of the existence of the pipe wall, wall modes characterize the behavior of perturbation with large azimuthal wave number.

Maslowe and Stewartson[3] studied the stability of inviscid pipe flow to perturbations of very large azimuthal wave number, and established that the prevailing modes are the wall modes in the limit of $m \to \infty$. Stewartson[11] analyzed the effect of the viscosity on ring modes and found that viscous effects come into play in higher order terms because the inviscid ring mode solution can satisfy the exact boundary conditions of the problem.

We study the wall mode when the viscosity is taken into account. Since the inviscid wall mode is close to the wall, where the no-slip condition is required but is not satisfied by the inviscid solution, it is expected that the viscous effect might be important in this case, at least in certain regions .

We are going to study the linear stability problem for large azimuthal wave number and large Reynolds number, i.e. both m and Re are large. In this case, the proper wall mode scalings are

$$\begin{aligned} r &= 1 - \frac{\eta}{(m^2+k^2)^{1/2}} \\ w &= i\bar{w} \\ p &= \frac{2\bar{p}}{m} \\ Re &= -\bar{Re}\frac{(m^2+k^2)^{3/2}}{2k} \\ \omega &= mq - \frac{2k\bar{\omega}}{(m^2+k^2)^{1/2}} \end{aligned} \tag{7}$$

The scaling for the radial variable means that the behavior of the wall mode is confined to a small distance to the wall comparable with the wave length of the perturbation. The scaling for the Reynolds number gives the balance between the viscous term and the inertia term. The form of the scaling for the complex

frequency is suggested by the numerical computations of the full linear stability problem. In above, a minus sign is introduced in places where k appears, for we know from the full linear stability problem that instability occurs only when $mk < 0$.

Upon substituting the above expressions into the linearized Navier-Stokes equations and the equation of continuity for the perturbation, and dropping the terms of order m^{-1} and smaller, we find that $\bar{w}$ should satisfy the following single equation, after $u, v, \bar{p}$ are eliminated.

$$LDLD\bar{w} - LL\bar{w} + LD\bar{w} - Q\bar{w} = 0 \qquad (8)$$

where

$$D = \frac{d}{d\eta}$$

$$L = \frac{i}{\bar{R}e}(D^2 - 1) - (\eta + \bar{\omega})$$

and

$$Q = -\frac{q(m + qk)}{k} \qquad (9)$$

which emerges as one of the independent parameters for the viscous wall mode.

The boundary conditions are

$$\bar{w} = D\bar{w} = D^2L\bar{w} - L\bar{w} = 0 \text{ at } \eta = 0 \qquad (10)$$

and

$$\bar{w} = D\bar{w} = D^2L\bar{w} - L\bar{w} = 0 \text{ as } \eta \to \infty \qquad (11)$$

Thus, we have established the formulation for the viscous wall modes. The governing equation takes a simpler form compared with the full problem, and the number of the independent parameters is reduced from *four* to *two*. Of these two parameters, $\bar{R}e$ and Q, Q measures the effect of rotation on the wall mode and $\bar{R}e$ measures the effect of viscosity on the wall mode. The solutions of above wall mode problem will give:

$$\bar{\omega} = \bar{\omega}(\bar{R}e, Q)$$

If $\mathrm{Im}(\bar{\omega})$ is less than zero, the flow is linearly stable; if $\mathrm{Im}(\bar{\omega})$ is positive, the flow is said to be linearly unstable.

4. Numerical Solution of Wall Mode Equations

In general, solutions of the wall mode equation have to be found numerically. Because the eigenvalue enters quadratically, this wall mode equation gives a nonlinear eigenvalue problem. This nonlinear eigenvalue problem is changed to a system of linear eigenvalue equations by letting

$$Y = L\bar{w} \qquad (12)$$

In Y, $\bar{w}$, the governing equations are

$$\begin{aligned} L(D^2 - 1)Y + 2DY - (Q - 2)\bar{w} &= 0 \\ Y - L\bar{w} &= 0 \end{aligned} \qquad (13)$$

and the boundary conditions are

$$\bar{w} = D\bar{w} = D^2Y - Y = 0 \quad \text{at } \eta = 0 \qquad (14)$$

$$\bar{w} = D\bar{w} = D^2Y - Y = 0 \quad \text{as } \eta \to \infty \qquad (15)$$

We employed a spectral method with Chebyshev polynomials as the basis functions to solve equations (13) - (15). Because the domain of definition extends to infinity, while Chebyshev polynomials are only defined over [-1, 1], the method of domain truncation was used to numerically truncate the domain of definition from $[0, \infty)$ to $[0, b]$ and the boundary conditions at infinity are replaced by

$$\bar{w} = D\bar{w} = D^2Y - Y = 0 \text{ at } \eta = b \qquad (16)$$

In the spectral method used, we write

$$\begin{aligned} \bar{w} &= \sum_{i=1}^{N} \bar{w}_i T_{i-1}(y) \\ Y &= \sum_{i=1}^{N} Y_i T_{i-1}(y) \end{aligned} \qquad (17)$$

where y is related to η by

$$y = 2\eta/b - 1.$$

Thus the domain of definition for y is [-1,1]. The reduction from the differential equations to a set of algebraic equations is made by a Galerkin-Tau projection — i.e. the Galerkin method is used to project the equations while the Tau method is used to enforce the boundary conditions on the spectral representations of the perturbation field. The Galerkin-Tau projection results in an set of algebraic equations, which are of the form of generalized eigenvalue problem with complex matrices.

Two methods are used in this study to find the eigenvalues and the eigenvectors of this complex generalized eigenvalue problem. One method uses the IMSL subroutine EIGZC which uses the QZ transformation to find all the eigenvalues and, optionally, all

the eigenvectors. The other method used is an inverse power iteration for the generalized eigenvalue problem developed by Kribus[12], which finds the eigenvalue closest to the initial guess and its corresponding eigenvector. The inverse power iteration is faster, so it is used whenever a good guess is available. The QZ is used to provide the starting values for the Inverse Power Iteration. It is also used when the phenomenon of mode jumping is suspected to occur.

Since the eigenfunctions decay exponentially as $\eta \to \infty$, $b = 10$ was found sufficient for most of the calculations. The number of terms in the Chebyshev representation, N, varies with $\bar{R}e$. For order one $\bar{R}e$, we must take $N = 60$, and $b = 10$ to achieve three digit accuracy in eigenvalue, and $O(10^{-4})$ accuracy for the eigenfunction. But when $\bar{R}e$ is large, the solution shows a behavior of boundary type for η near zero, i.e. near the wall of the pipe, and a large value of N is needed to resolved this region. The largest N needed for the parameter range covered here is 115.

There is a symmetry in the eigenvalue problem due to the replacement of the boundary conditions at infinity by the conditions at $\eta = b$. The solution is invariant under

$$\eta \quad \leftrightarrow \quad b - \eta$$

$$\bar{\omega} \quad \leftrightarrow \quad \bar{\omega}^* - b$$

$$\bar{w} \quad \leftrightarrow \quad \bar{w}^*$$

$$Y \quad \leftrightarrow \quad Y^*$$

where the star means the complex conjugate. This symmetry signifies that for a given solution, its image about $\eta = b/2$ is also a solution of this equation with the same growth rate. Apparently, this solution is a spurious mode in the sense that it is a solution of the differential equation after enforcing the boundary condition at finite b rather than the solution of the original differential equation defined over the infinite domain. This symmetry property can be used to check the resolution of the numerical solution of the algebraic problem, which should also exhibit this symmetry.

Extensive computations were carried out in the $(\bar{R}e, Q)$ plane. Fig 2 shows the imaginary part of the eigenvalue $\bar{\omega}$, which is proportional to the growth rate of the perturbation, vs. $\bar{R}e$ for some different values of Q. The eigenvalues shown are for $Q = 5$, 10, 20, 30, 40, 50 respectively, although numerical computations were carried out for a larger range of Q. The real part of the eigenvalue is shown in Fig 3. The growth rate increases as Q is increased, which means that rotation helps perturbations to extract energy from the

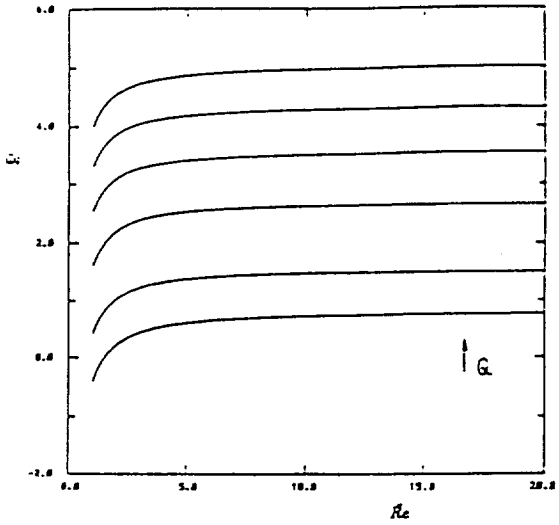

Figure 2: The imaginary part of the wall mode eigenvalues vs. $\bar{R}e$ for $Q = 5$, 10, 20, 30, 40, 50.

base flow. This result is in agreement with that of Pedley[1], who found that the maximum growth rate is 2.0 and is reached in the fast rotation limit. This is exactly the same as the upper bound for the growth rate for flow in the rotating pipe, as shown by Joseph and Carmi[5].

The growth rate increases with $\bar{R}e$. As $\bar{R}e$ gets large, the growth rate will increase. The eigenvalues seem to change smoothly as $\bar{R}e \to \infty$ and approach to the results found by Maslowe and Stewartson from their inviscid analysis. The limit of $\bar{R}e \to \infty$ will be analyzed asymptotically in the next section, and a comparison of the results with the inviscid case will be made.

Fig 4 shows the eigenfunction for $\bar{R}e = 2$, and $Q = 5$. The eigenfunction plotted is normalized such that its maximum modulus is 1 and its phase at the position of maximum modulus is 0. As in the eigenfunction plotted in Fig 1, the real part of the eigenfunction is drawn in solid line while the imaginary part of the eigenvalue is drawn in dotted line. To see the effect of increasing Q on the eigenfunction, we show in Fig 5 the eigenfunction for $\bar{R}e = 2$ and $Q = 20$. As Q increases, the eigenfunction is pushed outward, but this response is not very sensitive to Q. To see the effect of changing $\bar{R}e$, Fig 6 shows the eigenfunction for $\bar{R}e = 100$ and $Q = 5$. As $\bar{R}e$ increases, the eigenfunctions are pushed towards $\eta = 0$, i.e. toward the wall. The limit of $\bar{R}e \to \infty$ will be the further studied in the next section.

5. The Limit of $\bar{R}e \to \infty$

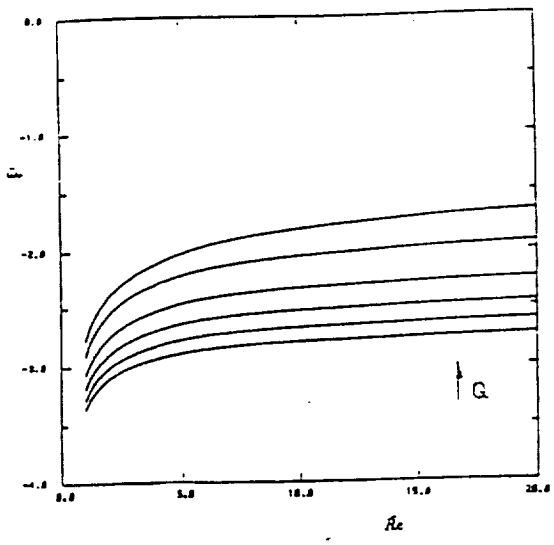

Figure 3: The real part of the wall mode eigenvalues vs. $\bar{R}e$ for $Q = 5$, 10, 20, 30, 40, 50.

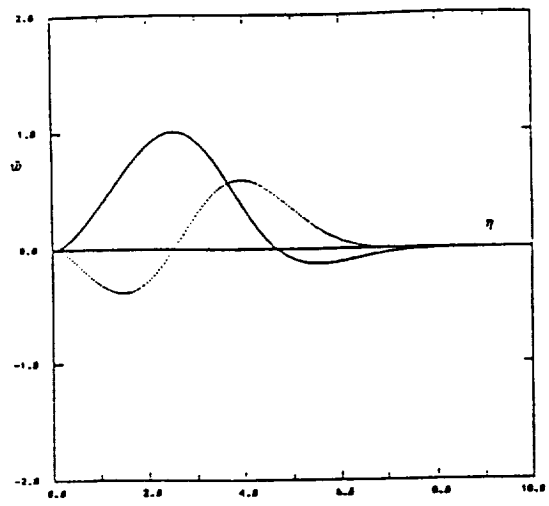

Figure 5: Wall mode eigenfunction, $\bar{R}e = 2, Q = 20$

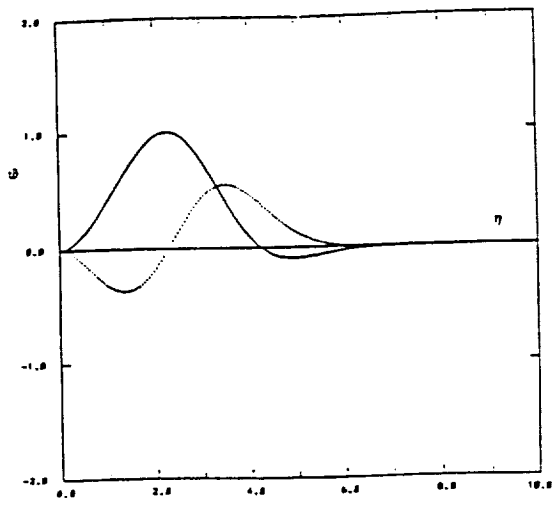

Figure 4: Wall mode eigenfunction, $\bar{R}e = 2, Q = 5$

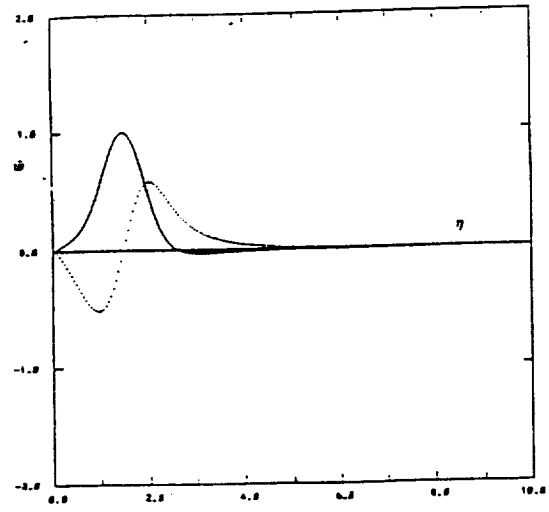

Figure 6: Wall mode eigenfunction, $\bar{R}e = 100, Q = 5$.

Maslowe and Stewartson[3] carried out the wall mode analysis for $m \gg 1$ for the inviscid case. One of the purposes of our viscous wall mode analysis is to see if the results of their inviscid analysis is the limit of the viscous analysis for large Reynolds number. We use a perturbation technique to address this question in this section.

For $\bar{R}e \gg 1$, $\bar{\omega}$ can be expanded formally by taking $\bar{R}e^{-1}$ as the small parameter, we write:

$$\bar{\omega} = W_0^o(\eta) + \bar{R}e^{-1}W_1^o(\eta) + ...$$

To leading order, the equation for W_0^o is:

$$D^2W_0^o - (1 + \frac{Q}{(\eta+\bar{\omega})^2})W_0^o = 0 \qquad (18)$$

with the following boundary conditions:

$$W_0^o(0) = 0 \qquad (19)$$

$$W_0^o(\eta \to \infty) \to 0 \qquad (20)$$

This poses the same eigenvalue problem that was studied by Maslowe and Stewartson, thus their solutions (both the eigenvalue and the eigenfunction) may be viewed, as might have been expected, as the first term in a formal outer expansion in inverse powers of $\bar{R}e$.

The outer solution thus found can satisfy all the boundary conditions at infinity since the outer solution decays exponentially as $\eta \to \infty$. But not all the boundary conditions at $\eta = 0$ can be satisfied. For example, $DW_0^o(0) \neq 0$. Thus, another (inner) solution of boundary type near $\eta = 0$ is needed.

The inner variable is found to be:

$$\zeta = \eta \bar{R}e^{1/2}$$

The inner expansion is assumed to be:

$$\bar{\omega} = \bar{R}e^{d}(W_0^i(\zeta) + \bar{R}e^{-1/2}W_1^i(\zeta) + ...)$$

where d is to be determined.

After substituted into the governing equation, the equation to leading order is found to be:

$$(\bar{D}^2 + \bar{\omega})^2\bar{D}^2W_0^i = 0 \qquad (21)$$

where

$$\bar{D} = \frac{d}{d\zeta}$$

The boundary conditions for the inner solution are:

$$W_0^i(0) = 0$$

$$\bar{D}W_0^i(0) = 0$$

$$(\bar{D}^2 + \bar{\omega})^2W_0^i(0) = 0 \qquad (22)$$

In addition, the solution is required to match the outer solution in the matched asymptotic sense.

The general solutions of the inner problem in the leading order can be found, and they are

$$W_0^i = \beta_1 \exp(\lambda_1\zeta) + \beta_2\zeta\exp(\lambda_1\zeta) + \beta_3\exp(\lambda_2\zeta) + \beta_4\zeta\exp(\lambda_2\zeta) + \beta_5 + \beta_6\zeta \qquad (23)$$

where

$$\lambda_{1,2} = \pm(i\bar{\omega})^{1/2}$$

and β_1, β_2, β_3, β_4, β_5, β_6 are constants to be determined by the boundary conditions and the matching conditions. $\bar{\omega}$ is given by the outer solution.

The boundary conditions at $\zeta = 0$ require that

$$\beta_1 + \beta_3 + \beta_5 = 0$$

$$\beta_1\lambda_1 + \beta_2 + \beta_3\lambda_2 + \beta_4 + \beta_6 = 0$$

$$2\lambda_1^3\beta_2 + 2\lambda_2^3\beta_4 = 0$$

As $\zeta \to \infty$, the inner solution must also match the outer solution. Near $\eta = 0$, the outer solution is, to leading order,

$$W_0^o = \alpha\eta$$

where $\alpha = DW_0^o(0) \neq 0$.

To carry out the matching, we need to know the behavior of W_0^i for large ζ. The behaviors of the exponential terms are determined by the sign of the real parts of λ_1, λ_2. Since λ_1, λ_2 are the square roots of $(i\bar{\omega})$, λ_1 is the negative of λ_2. In this study, we take

$$Re(\lambda_1) < 0$$

$$Re(\lambda_2) > 0$$

As $\zeta \to \infty$, the matching of the exponentially growing terms gives:

$$\beta_3 = 0$$

$$\beta_4 = 0$$

The exponentially small terms are immaterial, and the matching of the algebraic terms gives

$$\bar{R}e^{d}\beta_6\zeta = \alpha\eta \qquad (24)$$

which gives

$$d = -\frac{1}{2}$$

and

$$\beta_6 = \alpha$$

All the other constants can be determined, yielding

$$\beta_1 = -\alpha/\lambda_1$$

$$\beta_2 = 0$$

$$\beta_5 = \alpha/\lambda_1$$

The inner solution, to the leading order, is

$$W_0^i(\zeta) = \alpha(\zeta + \frac{1}{\lambda_1}(1 - \exp(\lambda_1\zeta))) \qquad (25)$$

Thus, we have the following composite solution to the leading order:

$$W_0^c = W_0^o(\eta) + W_0^i(\zeta) - \alpha\eta \qquad (26)$$

Thus, one sees that indeed, the solutions for the most unstable modes found by Maslowe and Stewartson are the correct limit when $\tilde{R}e \to \infty$, except in a thin layer near the wall of the pipe where the flow field is described by a viscous layer of the boundary layer type. The eigenvalues found are the same as for the inviscid case.

The above asymptotic analysis is confirmed by the numerical calculation. In Table 2, we present the eigenvalues for $\tilde{R}e = 100$ and in Table 3, we present the eigenvalues from the inviscid calculation for a few values of Q. It is seen that differences of the eigenvalues in these two cases are small. In Fig 7, we show the eigenfunction for $Q = 5.0$ from the inviscid calculation. It is seen that the general shape agrees with the viscous calculation presented in Fig 6. To see the existence of a thin viscous layer near the wall, we present in Fig 8a a blow-up of Fig 6, and in Fig 8b a blow up of Fig 7 near the wall. It is seen that flow fields near the wall are different, the viscous solution has a zero slope while the solution from the inviscid equation has a non-zero slope.

6. Discussion

We have examined the linear stability of rotating pipe flow to perturbations of large azimuthal wave number. It is found that when the azimuthal wave number is large, the nontrivial behaviors are concentrated near the wall of the pipe, so the prevailing variations are manifested as wall modes. The equations governing wall modes are found to contain two parameters $\tilde{R}e$ and Q, which measure the Reynolds number and swirl, respectively.

Table 2: Eigenvalue of viscous wall mode.

Q	eigenvalue ($\tilde{R}e = 100$)
5.0	(-0.14917D+01, 0.72752D+00)
10.0	(-0.18163D+01, 0.15096D+01)
20.0	(-0.21617D+01, 0.26668D+01)
30.0	(-0.23766D+01, 0.35755D+01)
40.0	(-0.25358D+01, 0.43505D+01)
50.0	(-0.26633D+01, 0.50384D+01)

Table 3: Eigenvalue of inviscid wall mode.

Q	eigenvalue ($\tilde{R}e = \infty$)
5.0	(-0.14142D+01, 0.68305D+00)
10.0	(-0.17476D+01, 0.14875D+01)
20.0	(-0.21038D+01, 0.26574D+01)
30.0	(-0.23247D+01, 0.35710D+01)
40.0	(-0.24877D+01, 0.43487D+01)
50.0	(-0.26181D+01, 0.50383D+01)

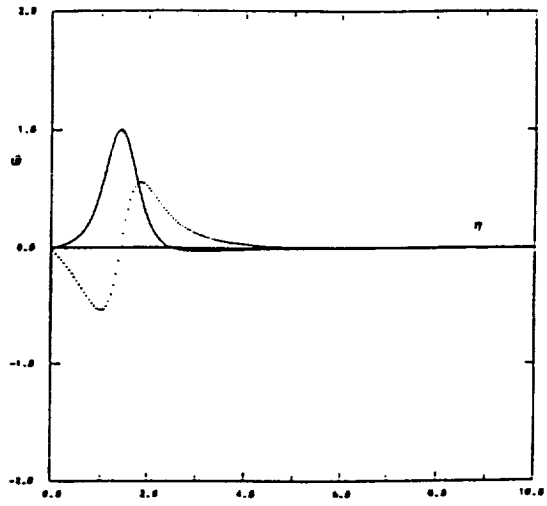

Figure 7: Wall mode eigenfunction for the inviscid case, $Q = 5$.

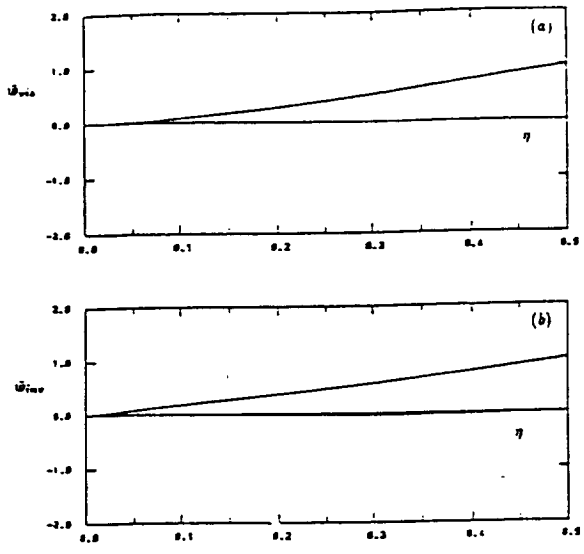

Figure 8: Comparison of the wall mode eigenfunctions near the wall. (a) the viscous solution at $\bar{R}e = 100$, (b) the inviscid solution.

For large azimuthal wave number, the wall mode is a distance $O(m^{-1})$ away from the wall. Viscous effects are confined to a layer with thickness of $O(Re^{-1/2})$ near the wall. The case treated here is when those two layers are of the same order, i.e. $Re = O(m^2)$. When $Re/m^2 \gg 1$, we would expect the solution to be mainly inviscid, as found by Maslowe and Stewartson, except in a thin viscous layer near the wall. This is indeed the case as shown both numerically and asymptotically.

The region for the rotation rate considered is $q = O(1)$. For large value of q, which corresponds to the fast rotation case, Pedley[4] shows that as Reynolds number is increased, the dominant mode is taken by perturbations of larger and larger values of m, the azimuthal wave number. In the limit of $Re \to \infty$, the azimuthal wave number for the dominant modes will also go to infinity, and these modes could be viewed as wall modes. Thus, our work here can be viewed as an extension of Pedley's work[1,4] to the region of $q = O(1)$.

Left unexamined is the case when the inviscid solution has a singularity, in which case the form of the expansion we assumed would break down. In the study of Maslowe and Stewartson, the leading mode is a neutral mode when $Q = 2$. For $Q > 2$, the leading mode is unstable, but there are still neutral modes. The neutral modes have a $1/(r - r_0)$ singularity, where r_0 is the location of the singularity. It is expected that a local viscous critical layer based on our viscous wall mode formulation would get rid of this singularity.

Acknowledgement

This work was supported by the Air Force Office of Scientific Research under contract AFOSR-89-0346 monitored by Dr. L. Sakell.

References

[1] T.J. Pedley. "On the instability of rapidly rotating shear flows to non-axisymmetric disturbances." *J. Fluid Mech.*, 31:603–607, 1968.

[2] S.A. Maslowe. "Instability of rigidly rotating flows to non-axisymmetric disturbances." *J. Fluid Mech.*, 74:303–317, 1974.

[3] S.A. Maslowe and K. Stewartson. "On the linear inviscid stability of rotating Poiseuille flow." *Phys. Fluids*, 25:1517–1523, 1982.

[4] T.J. Pedley. "On the instability of viscous flow in a rapidly rotating pipe." *J. Fluid Mech.*, 35:97–115, 1969.

[5] D.D. Joseph and S. Carmi. "Stability of Poiseuille flow in pipes, annuli, and channels." *Quart. Appl. Math.*, 26:575–599, 1969.

[6] F.W. Cotton and H. Salwen. "Linear stability of rotating Hagen-Poiseuille flow." *J. Fluid Mech.*, 108:101–125, 1981.

[7] K. Stewartson, T.W. Ng, and S.N. Brown. "Viscous center modes in the stability of swirling Poiseuille flow." *Phil. Trans. Roy.*, 324:473–512, 1988.

[8] G.K. Batchelor and A.E. Gill. "Analysis of the stability of axisymmetric jets." *J. Fluid Mech.*, 14:529–551, 1962.

[9] Z. Yang. *Two theoretical studies of stability of swirling flows.* PhD Thesis, Cornell University, 1990.

[10] S. Leibovich and K. Stewartson. "A sufficient condition for the instability of columnar vortices." *J. Fluid Mech.*, 126:335–356, 1983.

[11] K. Stewartson. "The stability of swirling flow at large Reynolds number when subject to disturbances of large azimuthal wavenumber." *Phys. Fluids*, 25:1953–1957, 1982.

[12] A. Kribus. "Computation of leading eigenspaces for generalized eigenvalue problems." *Trans. of the 7th Army Conf. on Appl. Math and Comp.*, 1990.